Electronic Supplementary Material (ESI) for Journal of Materials Chemistry A.

Electronic Supplementary Information

Three-Dimensional Hierarchically Porous Mo_2C architecture: Salt-Templated Synthesis, Robust Electrocatalyst and Anode Materials towards Hydrogen Evolution Reaction and Lithium Storage

Tao Meng[1], Lirong Zheng[2], Jinwen Qin[1], Di Zhao[1], and Minhua Cao*[,1]

[1]Key Laboratory of Cluster Science, Ministry of Education of China, Beijing Key Laboratory of Photoelectronic/Electrophotonic Conversion Materials, School of Chemistry and Chemical Engineering, Beijing Institute of Technology, Beijing 100081, P. R. China.

[2]Beijing Synchrotron Radiation Laboratory, Institute of High Energy Physics, Chinese Academy of Sciences, Beijing 100049, P. R. China.

* Corresponding author. E-mail: caomh@bit.edu.cn .

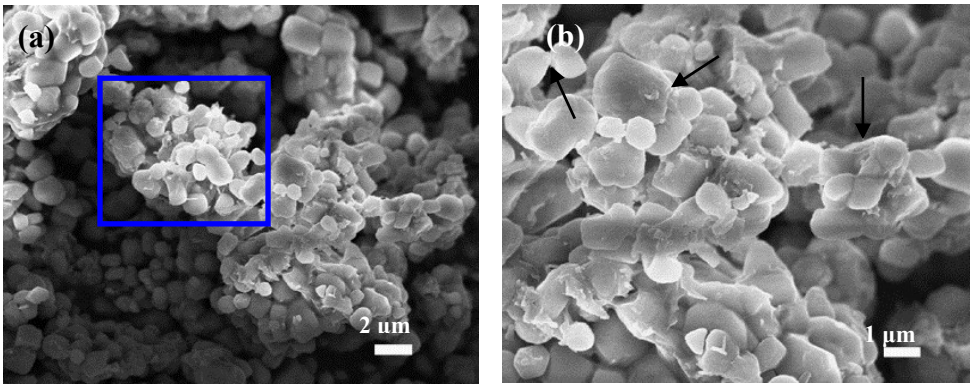

Fig. S1 FESEM image of NaCl@PVP-[$(NH_4)_6Mo_7O_{24}$] for step 3 in scheme 1.

As the shown Fig. S 1a, the 3D unit (*e.g.* marked by the blue box) was structured by many nanoparticles. Further, according to the enlarged SEM image (Fig. S 1b), we can find that there is an ultrathin film on the surface of the particle (*e.g.* marked by the arrows). Based on this fact, we concluded that "Second, this solution was subjectd to freeze-drying, during which NaCl recrystallized to form cubes and at the same time an ultrathin PVP-$(NH_4)_6Mo_7O_{24}$ complex film was uniformly coated on the surface of NaCl cubes to self-assemble into a 3D framework (3D-NaCl@PVP-$(NH_4)_6Mo_7O_{24}$)".

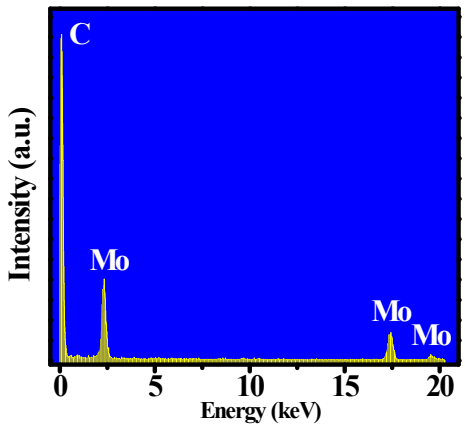

Fig. S2 The EDS pattern of 3DHP-Mo_2C.

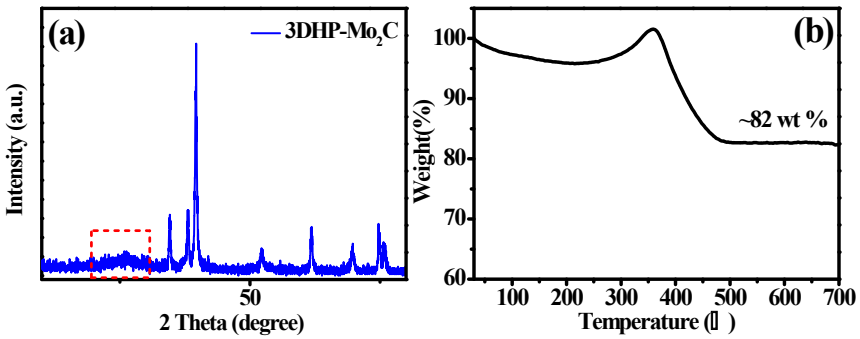

Fig. S3 (a) XRD pattern of 3DHP-Mo_2C. (b) TGA curve of 3DHP-Mo_2C from the room temperature to 700 °C with a heating rate of 20 °C min^{-1} in air.

Fig. S3b: For TGA curve, the initial weight gain above 200 °C is due to the gradual oxidation of Mo_2C to MoO_3, followed by a significant weight loss caused by the combustion of carbon. Assuming that the sample is composed of stoichiometric Mo_2C and carbon, and it converts to only MoO_3 after being heated to 500 °C, the contents of Mo_2C and carbon are estimated according to the following equation:

$$m\ (Mo_2C) = 82\ wt\ \% * M(Mo_2C)/2*M(MoO_3) = 82\ wt\ \% *204/(2*144) = 58\ wt\ \%$$

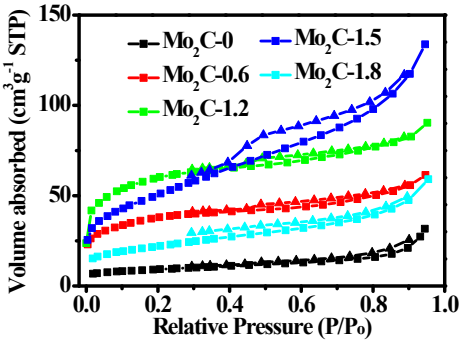

Fig. S4 N_2 adsorption-desorption isotherms of Mo_2C-X (X = 0.0, 0.6, 1.5, and 1.8 g, and X stands for the mass of NaCl template).

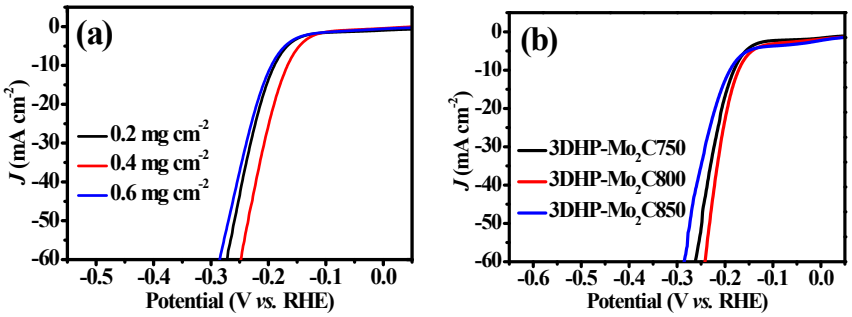

Fig. S5 (a) Polarization curves of 3DHP-Mo_2C with different loadings on a glassy carbon (GC) electrode. (b) Polarization curves of 3DHP-Mo_2C obtained at 750, 800 and 850 °C, respectively, in 0.5 M H_2SO_4.

Fig. S5b: Compared with 3DHP-Mo_2C800, 3DHP-Mo_2C750 and 3DHP-Mo_2C850 samples exhibit slightly inferior activity towards HER. And the reason may be either the insufficient crystallinity at the low temperature or the aggregation of Mo_2C nanocrystallites at the high temperature.

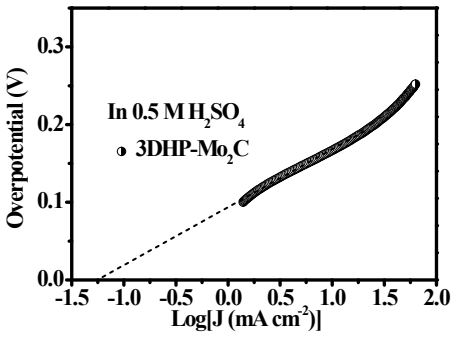

Fig. S6 Calculation of exchange current density for the 3DHP-Mo_2C in 0.5 M H_2SO_4 by extrapolation method.

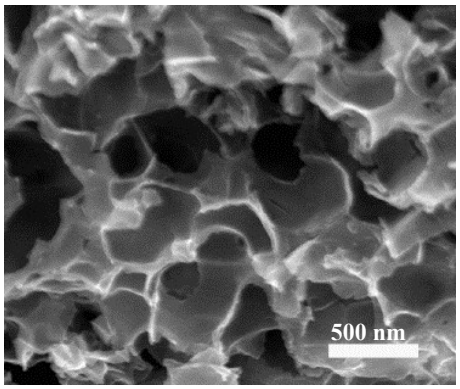

Fig. S7 FE-SEM image of 3DHP-Mo_2C after stability test for HER in 0.5 M H_2SO_4.

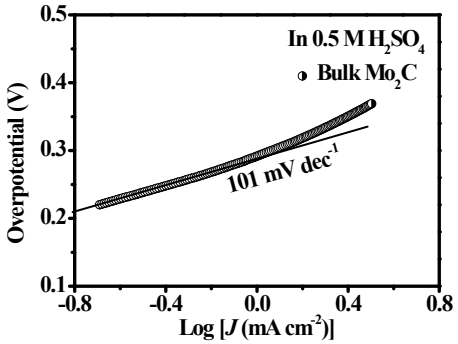

Fig. S8 Tafel plots of the bulk Mo_2C in 0.5 M H_2SO_4

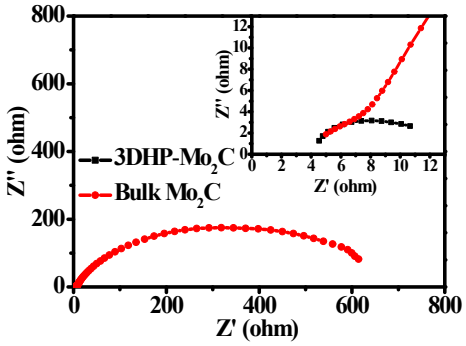

Fig. S9 EIS spectra tested at -0.3 V *vs.* RHE for 3DHP-Mo_2C and bulk Mo_2C in 0.5 M H_2SO_4.

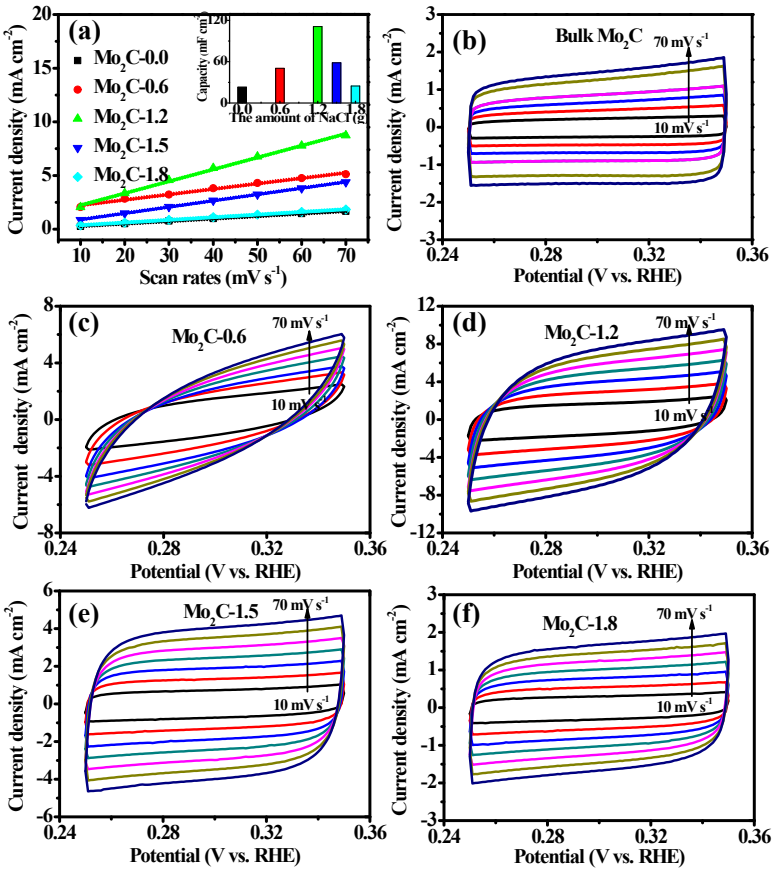

Fig. S10 (a) Plots of the capacitive currents at 0.33 V *vs.* RHE as a function of scan rate for Mo_2C-X (X stands for the mass of the NaCl template). CVs of Mo_2C-0.0 (b), Mo_2C-0.6 (c), Mo_2C-1.2 (d), Mo_2C-1.5 (e), and Mo_2C-1.8 (f) measured at different scan rates from 10 to 70 mV s^{-1} in 0.5 M H_2SO_4.

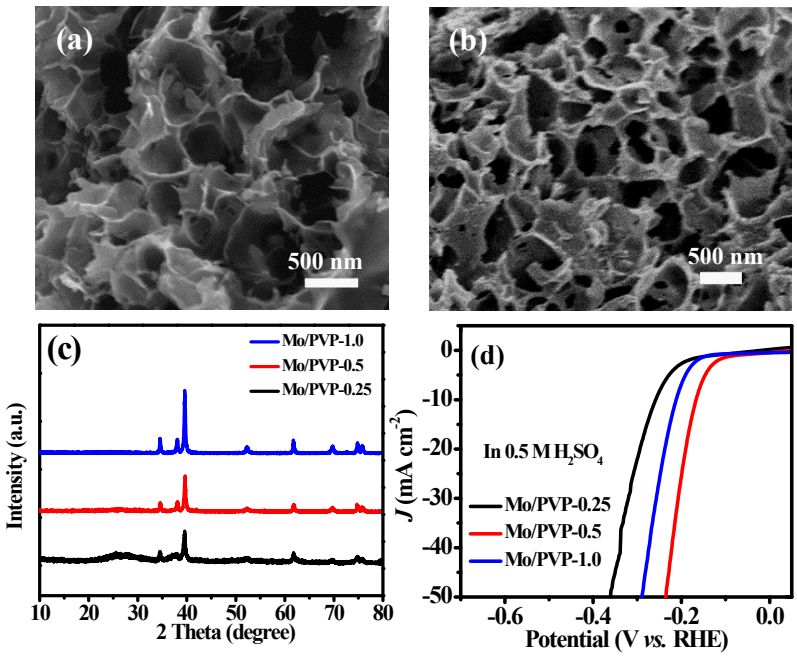

Fig. S11 FE-SEM images of Mo/PVP-0.25 (a) and Mo/PVP-1.0 (b). (c) Corresponding XRD patterns. (d) Polarization curves for Mo_2C prepared with different mass rates of $(NH_4)_6Mo_7O_{24}$ to PVP (Mo/PVP).

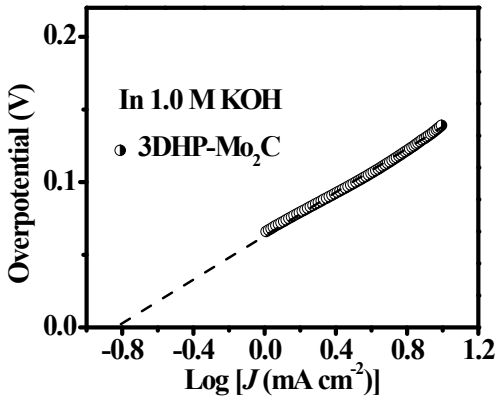

Fig. S12 Calculation of the exchange current density for 3DHP-Mo_2C in 1.0 M KOH by extrapolation method.

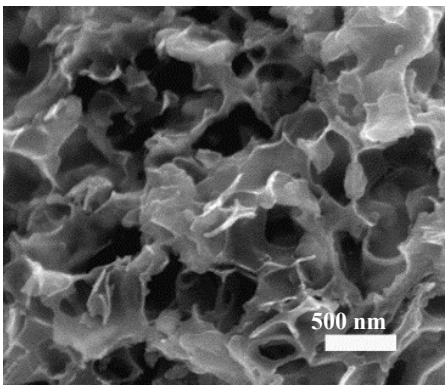

Fig. S13 FE-SEM image of 3DHP-Mo_2C after stability test for HER in alkaline solution.

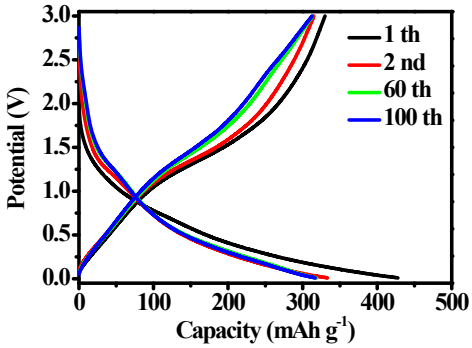

Fig. S14 Charge-discharge profiles of bulk Mo_2C for the 1st, 2nd, 60th, and 100th cycles at a current density of 0.1 A g^{-1}

Table S1 Comparison of HER performance in acidic media for 3DHP-Mo_2C with other non-noble metal electrocatalysts.

Catalysts	Current density (j, mA cm^{-2})	η at the corresponding j (mV)	Tafel slope (mV dec^{-1})	J_0 (mA cm^{-2})	Ref.
3DHP-Mo_2C	**10** **20**	**166** **190**	**75**	**0.287**	**This work**
MoDCA-5	10	78	41	0.178	1
MoDCA-2	10	205	68	0.017	
Mo_2C@NC	10	60	60	0.096	2
Mo_2C-NCNTs	10	147	71	0.1146	3
Mo_2C-RGO	10	130	57.3	N.A. [a]	4
Mo_2C Nanotubes	10 20	172 197	62	0.017	5
Mo_2C/GCSs	10	200	62.6	0.0125	6
MoC_x Nano-Octahedrons	1 10	87 142	53	0.023	7
MoB Microparticles	10	>200 [b]	55	0.0014	8
$V_{0.09}Mo_{0.91}S_2$	10	>200	69	N.A.	9
Amorphous MoP Nanoparticles	10 20	110 140	45	0.12	10
Atomically-Thin MoN Nanosheets	10	>200	90	0.08375	11
Defect-Rich MoS_2 Ultrathin NSs	13	200	50	0.00891	12
C_3N_4@NG	10	240	51.5	0.00035	13

a : not given.

b: data were directly collected from the polarization curves in the reported articles.

Table S2 Comparison of HER performance in alkaline media for 3DHP-Mo_2C with other non-noble metal electrocatalysts.

Catalysts	Current density (j, mA cm^{-2})	η at the corresponding j (mV)	Tafel slope (mV dec^{-1})	J_0 (mA cm^{-2})	Ref.
3DHP-Mo_2C	**10** **20**	**139** **174**	**71**	**0.441**	**This work**
Mo_2C@NC	10	60	N.A.	N.A.	2
Mo_2C Nanotubes	10 20	112 127	55	0.087	5
MoC_x Nano-Octahedrons	1 10	92 151	59	0.029	7
MoP Nanoparticles	10	~130	48	0.046	14
MoB Microparticles	10	>210	59	0.002	8
MoS_2 NS Arrays	10	190	100	N.A.	15
CoP-MNA	10 100	54 121	51	0.857	16
CoO_x/N-Doped Carbon Hybrids	10	232	115	N.A.	17
CoP Nanowire Arrays	1 10	115 209	129	N.A.	18
FeP NAs/CC	10	218	146	0.5	19

Table S3 Comparison of the capacity of 3DHP-Mo_2C with reported molybdenum carbide-based materials

Samples	Current density ($A\ g^{-1}$)	Cycle number (n)	Capacity ($mAh\ g^{-1}$)	Ref.
3DHP-Mo_2C	**0.1** **0.3**	**100** **100**	**927.4** **654.3**	**This work**
Mo_2C-C Nanospheres	0.1	50	672.7	20
Mo_2C/GR	0.1	100	813	21
HP-Mo_2C-C	0.1	100	1196.8	22
$MoC_{0.654}$@CNS	0.5	680	815	23
Mo_2C Nanoparticles	0.1	50	658	24
MoO_2/Mo_2CHeteronanotubes	0.2	20 (140)	610 (790)	25
MoO_2/Mo_2C/C Spheres	0.1	100	~ 800	26
MoO_2-Mo_2C-C	0.2	50	838	27
Co_3ZnC/C-N	0.1	60	968.1	28
Fe/Fe_3C-CNFs	0.2	70	~500	29

References

1 R. G. Ma, Y. Zhou, Y. F. Chen, P. X. Li, Q. Liu, and J. C. Wang, *Angew. Chem. Int. Ed.,* 2015, **54**, 14723-14727.

2 Liu, Y. P.; Yu, G. T.; Li, G. D.; Sun, Y. H. Asefa, T.; Chen, W.; Zou, X. X. *Angew. Chem. Int. Ed.,* 2015, **54**, 10752-10757.

3 K. Zhang, Y. Zhao, D. Y. Fu, and Y. J. Chen, *J. Mater. Chem. A,* 2015, **3**, 5783-5788.

4 L. F. Pan, Y. H. Li, S. Yang, P. F. Liu, M. Q. Yu, and H. G. Yang, *Chem. Commun.,* 2014, **50**, 13135-13137.

5 F. X. Ma, H. B. Wu, B. Y. Xia, C. Y. Xu, and X. W. Lou, *Angew. Chem. Int. Ed.,* 2015, **54**, 15395-15399.

6 W. Cui, N. Y. Cheng, Q. Liu, C. J. Ge, A. M. Asiri, and X. P. Sun, *ACS Catal.* 2014, **4**, 2658-2661.

7 H. B. Wu, B. Y. Xia, L. Yu, X. Y. Yu, and X. W. Lou, *Nat. Commun.* 2015, **6**, 6512.

8 H. Vrubel, and X. L Hu, *Angew. Chem. Int. Ed.,* 2012, **124**, 12875-12878.

9 X. Sun, J. Dai, Y. Q. Guo, C. Z. Wu, F. T. Hu, J. Y. Zhao, X. C. Zeng, and Y. Xie, *Nanoscale,* 2014, **6**, 8359-8367.

10 J. M. McEnaney, J. C. Crompton, J. F. Callejas, E. J. Popczun, A. J. Biacchi, N. S. Lewis, and R. E. Schaak, *Chem. Mater.* 2014, **26**, 4826-4831.

11 J. F. Xie, S. Li, X. D. Zhang, J. J. Zhang, R. X. Wang, H. Zhang, B. C. Pan, and Y. Xie, *Chem. Sci.,* 2014, **5**, 4615-4620.

12 J. F. Xie, H. Zhang, S. Li, R. X. Wang, X. Sun, M. Zhou, J. F. Zhou, X. W. Lou, and Y. Xie, *Adv. Mater.* 2013, **25**, 5807.

13 Y. Zheng, Y. Jiao, Y. H. Zhu, L. H. Li, Y. Han, Y. Chen, A. J. Du, M. Jaroniec, and S. Z. Qiao, *Nat. Commun.* 2014, **5**, 3783.

14 P. Xiao, M. Sk, L. Thia, X. M. Ge, R. Lim, J. Y. Wang, K. Lim, and X. Wang, *Energy Environ. Sci,* 2014, **7**, 2624-2629.

15 J. L. Shi, and J. M. Hu, *Electrochim. Acta.* 2015, **168**, 256-260.

16 Y. P. Zhu, Y. P. Liu, T. Z. Ren, and Z. Y. Yuan. *Adv. Fun. Mater.,* 2015, **25**, 7337-7347.

17 H. Y. Jin, J. Wang, D. F. Su, Z. Z. Wei, Z. F. Pang, and Y. Wang, *J. Am. Chem. Soc.,* 2015, **137**, 2688-2694.

18 J. W. Tian, Q. Liu, A. M. Asiri, and X. P. Sun, *J. Am. Chem. Soc.,* 2014, **136**, 7587-7590.

19 Y. H. Liang, Q. Liu, A. M. Asiri, X. P. Sun, and Y. G. Luo, *ACS Catal.,* 2014, **4**, 4065-4069.

20 Q. Gao, X. Y. Zhao, Y. Xiao, Di. Zhao, and M. H. Cao, *Nanoscale,* 2014, **6**, 6151-6157.

21 B. B. Wang, G. Wang, and H. Wang, *J. Mater. Chem. A,* 2015, **3**, 17403-17411.

22 Y. Xiao, L. R. Zheng, and M. H. Cao, *Nano Energy,* 2015, **12**, 152-160.

23 J. X. Zhu, K. Sakaushi, G. Clavel, M. Shalom, M. Antonietti, and T. P. Fellinger, *J. Am. Chem. Soc.,* 2015, **137**, 5480-5485.

24 R. R. Li, S. G. Wang, W. Wang, and M. H. Cao, *Phys. Chem. Chem. Phys.,* 2015, **17**, 24803-24809.

25 H.J. Zhang, K. X. Wang, X. Y. Wu, Y. M. Jiang, Y. B. Zhai, C. Wang, X. Wei, and J. S. Chen, *Adv. Fun. Mater.,* 2014, **24**, 3399-3404.

26 M. Ihsana, H. Q. Wang, S. R. Majidc, J. P. Yang, S. J. Kennedyd, Z. P. Guo, and H. K. Liu. *Carbon,* 2016, **96**, 1200-1207.

27 Y. P. Zhua, S. F. Wang, Y. J. Zhong, R. Cai, L. Li, and Z. P. Shao; *J. Power. Sources,* 2016, **307**, 552-560.

28 Y. Xiao, P. P. Sun, and M. H. Cao, *ACS Nano,* 2014, **8**, 7846-7857.

29 J. X. Lia, W. W. Wen, G. G. Xu, M. Z. Zou, Z. G. Huang, and L. H. Guan, *Electrochimica Acta,* 2015, **153**, 300-305.